

## Research Article

# Effect of Alumina Dopant on Transparency of Tetragonal Zirconia

**Haibin Zhang,<sup>1</sup> Zhipeng Li,<sup>2</sup> Byung-Nam Kim,<sup>1</sup> Koji Morita,<sup>1</sup>  
Hidehiro Yoshida,<sup>1</sup> Keijiro Hiraga,<sup>1</sup> and Yoshio Sakka<sup>1</sup>**

<sup>1</sup> Advanced Materials Processing Unit, National Institute for Materials Science, 1-2-1 Sengen, Tsukuba, Ibaraki 305-0047, Japan

<sup>2</sup> Global Research Center for Environment and Energy based on Nanomaterials Science (GREEN),  
National Institute for Materials Science, 1-1 Namiki, Tsukuba, Ibaraki 305-0044, Japan

Correspondence should be addressed to Haibin Zhang, hzbzhang1978@gmail.com

Received 28 October 2012; Accepted 15 December 2012

Academic Editor: Xijin Xu

Copyright © 2012 Haibin Zhang et al. This is an open access article distributed under the Creative Commons Attribution License, which permits unrestricted use, distribution, and reproduction in any medium, provided the original work is properly cited.

Aiming to characterize the effect of alumina dopant on transparency, powders of yttria stabilized tetragonal zirconia doped with alumina (TZ-3Y-E) are used as starting material to fabricate transparent tetragonal  $\text{ZrO}_2$  by high-pressure spark plasma sintering (HP-SPS). However, low transparency of the resultant TZ-3Y-E specimens does not suggest a beneficial effect of alumina dopant although nanometric grains and high density have been achieved. The mechanism is analyzed by comparing with the results of as-sintered yttria stabilized tetragonal zirconia without alumina dopant.

## 1. Introduction

Yttria stabilized tetragonal zirconia polycrystal (Y-TZP) possesses many salient properties, such as high strength, toughness, wear resistance, chemical resistance, and biocompatibility, which make it as a promising candidate for various structural and biomedical applications [1]. As a hard-to-sinter ceramic, polycrystalline Y-TZP usually is opaque even after high-temperature sintering mainly because of the existence of residual pores. Such pores can significantly scatter incident light and deteriorate optical properties. In addition, nanometric microstructure is crucial to achieve good transparency for Y-TZP since this material has serious birefringent scattering (one order of magnitude higher than that of alumina) [2].

Very recently, Krell and coworkers propose a model based on Mie theory to quantitatively describe the scattering behavior in Y-TZP [2]. This model points out that the in-line transmittance of 50% at the visible wavelength range is expected as the grain size  $<40$  nm for a pore-free Y-TZP with 1 mm thickness [2]. This can account for the previous experimental results of the low transparency of Y-TZP [2–5], since such fine grains are not attained. On the other hand, this model reveals the weak birefringent scattering in the infrared (IR) range as grain sizes less than 200 nm.

This prediction is verified by the experimental results [2, 6]. Nanometric (115 nm) and dense tetragonal  $\text{ZrO}_2$  was fabricated by Klimke et al. [2] using hot isotropic pressing (HIP). The 0.5 mm thickness specimen exhibited the maximum theoretical value of in-line transmittance (77%) in the IR region of 4–5  $\mu\text{m}$ . The present authors [6] prepared nanograined (80 nm) and dense tetragonal zirconia using high-pressure spark plasma sintering (HP-SPS). In-line transmittance of a 1.5 mm thick sample approached 81–87% of the theoretical value in the wavelength of 3–5  $\mu\text{m}$ . Meanwhile, tetragonal  $\text{ZrO}_2$  showed the longest cutoff wavelength for high-strength transparent ceramics. These results highlight the great potential of this ceramic applied for durable infrared windows [2, 6].

It has been well established the beneficial effect of alumina dopant for sintering Y-TZP. The densification behavior and microstructural evolution during sintering of Y-TZP doped with alumina have been investigated by several researchers [7–13]. For example, Matsui et al. [7] found that the increase of alumina concentration could enhance the densification rate of Y-TZP, which was due to the improvement of apparent frequency-factor term in rate constant. Consequently, Y-TZP doped with alumina is highly expected as a superior raw material for fabricating transparent tetragonal zirconia.

This speculation was tested in the present study. Nanopowders of Y-TZP doped with alumina were used to prepare transparent tetragonal zirconia by high-pressure spark plasma sintering (HP-SPS). The effect of alumina dopant on transparency was analyzed with the comparison of that in pure Y-TZP nanopowders.

## 2. Experimental Procedure

**2.1. Sample Preparation.** The starting materials were commercial 3 mol%  $\text{Y}_2\text{O}_3$  stabilized  $\text{ZrO}_2$  powders with 0.3 mol%  $\text{Al}_2\text{O}_3$  dopant (TZ-3Y-E, Tosoh Corporation, Tokyo, Japan) and 3 mol%  $\text{Y}_2\text{O}_3$  doped  $\text{ZrO}_2$  powders (TZ-3Y, Tosoh Corporation, Tokyo, Japan). These two commercial powders were consolidated directly using a spark plasma sintering machine (SPS-1050, SPS Syntex Inc., Kawasaki, Japan) in vacuum ( $10^{-3}$  Torr) to obtain dense bulk specimens. The applied pressure was 400 MPa [6] and the heating rate was  $10^\circ\text{C}/\text{min}$ . Sintering resulted in disk samples of 10 mm diameter and 1.3 mm thickness. The as-sintered samples were annealed at  $900^\circ\text{C}$  for 4 hours in air.

**2.2. Optical Characterization.** For measuring optical properties, both surfaces of the as-prepared disks were mirror-polished using diamond slurry. The total forward transmittance, in-line transmittance, and reflection were measured with a double-beam spectrophotometer (SolidSpec-3700DUV, Shimadzu Co. Ltd., Kyoto, Japan) equipped with an integrating sphere. The distance between the sample and the detector was about 55 cm. For in-line transmittance measurements, a 3 mm pinhole was placed in front of the detector selecting only the in-line transmitted portion of the incident light (5 mm diameter). This setup allowed us to measure the “real in-line transmittance” [14].

The measured total forward transmittance ( $T$ ) and in-line transmittance ( $I$ ) could be expressed as the following formulas [15, 16]:

$$T = (1 - R) \exp(-\alpha t), \quad (1)$$

$$I = (1 - R) \exp[-(\alpha + \beta)t] = T \exp(-\beta t), \quad (2)$$

where  $R$  is the measured reflection,  $\alpha$  is the absorption coefficient,  $t$  is the sample thickness, and  $\beta$  is the scattering coefficient. The absorption coefficient and scattering coefficient could be calculated from (1) and (2), respectively.

**2.3. Microstructure Observation.** For transmission electron microscope (TEM) observations, a  $500\text{ }\mu\text{m}$  thick slab was cut by a low-speed diamond cutter, mechanically polished down to  $100\text{ }\mu\text{m}$ , and further thinned with an Ar ion-milling machine. The TEM observations were performed using a JEOL-2010F microscope (JEOL Ltd., Akishima, Tokyo, Japan) operated at 200 kV. The grain size was measured by evaluating the average cross-sectional area per grain under the assumption of spherical grains. Because the samples had small pores and low porosity, grain boundary grooving caused by etching would distort the SEM images. Therefore,

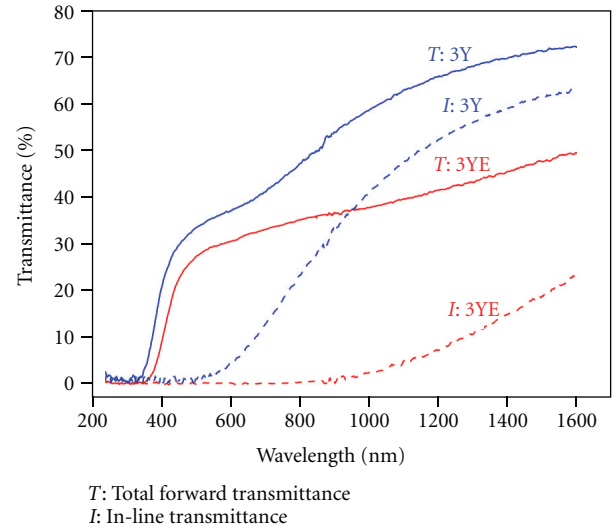


FIGURE 1: Typical total forward transmittance and in-line transmittance spectra of the yttria stabilized tetragonal zirconia without (3Y) and with alumina dopant (3YE). These two specimens were sintered for 10 min at  $1050^\circ\text{C}$  under the pressure of 400 MPa by means of SPS. The post-SPS annealing was conducted at  $900^\circ\text{C}$  for 4 hours in air. The samples analyzed in Figures 2 to 5 were fabricated at the same conditions. The thickness of these two samples was 1 mm.

the porosity was measured by TEM, as an average value over five images.

## 3. Results and Discussion

It is possible to fabricate low translucent tetragonal zirconias using the TZ-3Y-E powders by means of high-pressure spark plasma sintering (HP-SPS) under the pressure of 400 MPa. The study of high pressure SPS of transparent TZ-3Y can be found elsewhere [6]. The optimum sintering temperature presents at  $1050^\circ\text{C}$  for TZ-3Y-E specimens fabricated at 1000 to  $1200^\circ\text{C}$ , thus we restrict our measurements and discussion to this sample in the following. The appearance of this sample is dark (not shown here). The dark appearance is usually attributed to color centers (oxygen vacancies with trapped electrons) [4–6, 16, 17], which are easily produced in zirconia under thermal reduction or electroreduction conditions [4–6, 16, 17]. The SPS process actually provides both conditions because high-temperatures vacuum and graphite dies yield thermal reduction, and electric current may result in electroreduction. We have observed the similar phenomenon in the study of transparent TZ-3Y [6]. After SPS processing, annealing is conducted at  $900^\circ\text{C}$  for 4 hours in air to reduce color centers of the TZ-3Y-E and TZ-3Y samples.

Figure 1 shows typical in-line transmittance and total forward transmittance spectra of TZ-3Y-E and TZ-3Y specimens. It can be observed that, in contrast to the expectation, the addition of alumina dopant actually results in worse optical properties of total forward transmittance and in-line transmittance. In addition, since the total forward transmittance contains the in-line transmittance and the

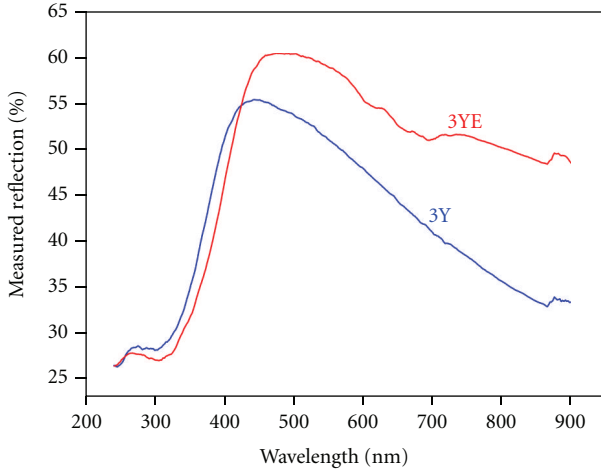


FIGURE 2: Dependence of the measured reflection of the yttria stabilized tetragonal zirconia without (3Y) and with alumina dopant (3YE). The thickness of these two samples was 1 mm.

forward scattering light, the increase of the total forward transmittance implies the existence of light scattering in the present samples. This scattering effect originates from residual pores and birefringence due to a tetragonal structure.

The dependence of light reflection on wavelength is represented in Figure 2. The reflection becomes more pronounced by the addition of alumina dopant. Here, the measured value consists of the intrinsic reflection losses at the front and back surfaces of the sample and back scattering from residual pores and birefringence. The intrinsic reflection should be independent of adding extremely low concentration of alumina dopant; therefore, only the increase of back scattering enhances the reflection of the TZ-3Y-E sample. It should be noted that grain boundary reflection, that is contribution from birefringence to back scattering, cannot be neglected in tetragonal zirconia because of its high birefringence. The maximum reflectivity  $R_{\max}$  by  $m$  grain boundaries is given by [18]

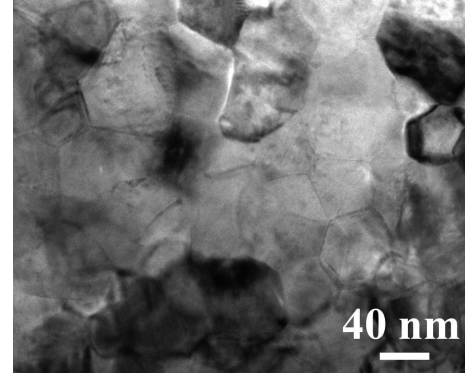
$$R_{\max} \approx 1 - (1 - R_{\perp})^m, \quad (3)$$

where  $R_{\perp}$  is the reflectivity for perpendicular incidence.  $R_{\perp}$  can be calculated using

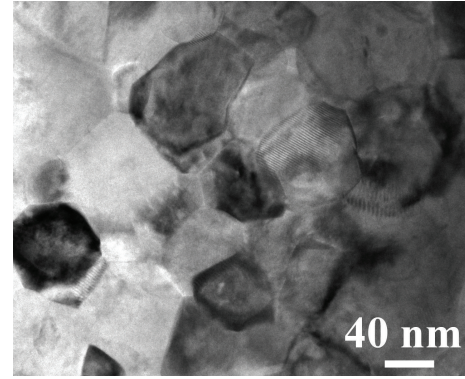
$$R_{\perp} = \frac{\Delta n^2}{(n_1 + n_2)^2}, \quad (4)$$

where  $n_1$  and  $n_2$  are the refractive indexes of two neighboring grains, and  $\Delta n$  is the refractive index difference [18]. For a 1 mm thick zirconia sample with grain size of 80 nm (see Figure 3), a light beam passes 1250 grain boundaries assuming that 10% grain boundaries are perpendicular to this beam. From (3), the reflectivity can be approximately estimated as 6% using  $\Delta n = 0.03$ ,  $n_1 = 2.16$ , and  $n_2 = 2.19$  [19]. Therefore, the contribution from the reflection at grain boundaries to back scattering of incident light cannot be omitted in tetragonal zirconia.

Figure 3 represents typical bright field TEM images for the microstructure of annealed TZ-3Y-E and TZ-3Y



(a)



(b)

FIGURE 3: Bright-field TEM images of the yttria stabilized tetragonal zirconia without (a) and with alumina dopant (b).

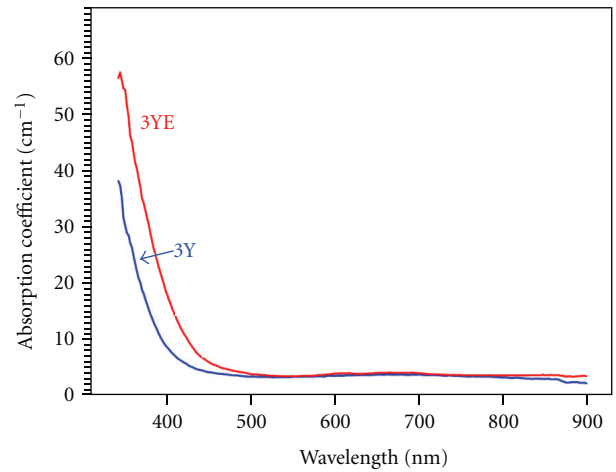


FIGURE 4: Absorption coefficients of the yttria stabilized tetragonal zirconia without (3Y) and with alumina dopant (3YE).

specimens. Fine intergranular pores are very rarely observed in TEM, indicating the extremely high density of the resultant specimens. It is hard to distinguish the difference of porosity between these two samples, and the porosity is estimated to be less than 0.05%. Meanwhile, similar mean grain size of about 80 nm is achieved for both specimens.

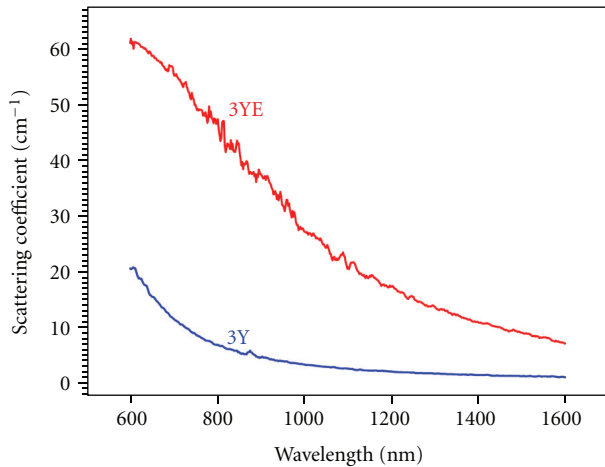


FIGURE 5: Scattering coefficients of the yttria stabilized tetragonal zirconia without (3Y) and with alumina dopant (3YE).

Figure 4 is the variation of the absorption coefficient on wavelength. It can be seen that the absorption coefficient of the TZ-3Y-E sample is slightly stronger than that of the TZ-3Y sample. This result indicates that more color centers are produced in the TZ-3Y-E sample. In fact, the dissolution of alumina dopant in zirconia promotes the production of color centers, and the defect reaction is written as the following [7]:



Meanwhile, alumina dopant just promotes the limited formation of color centers because of its low dissolution in zirconia [7]. Nevertheless, color centers cannot account for the low transmittance of the TZ-3Y-E sample because difference of absorption coefficients only occurs in short wavelength.

Figure 5 shows the dependence of the scattering coefficient on wavelength. Much higher scattering coefficient presented in the TZ-3Y-E sample obviously deteriorates the transparency. In the present zirconia samples, light scattering is induced by residual pores and birefringence. The similar porosity (Figure 3) implies that the difference in scattering coefficient only results from the different birefringence of these two samples. On the other hand, the similar grain size (Figure 3) cannot cause different birefringence of these two samples.

In fact, it is well known that most of alumina dopants distribute along grain boundaries of zirconia because of the very limited solubility, which has been clearly observed by Matsui et al. using STEM combined with nanoprobe electron dispersive X-ray spectroscopy [20]. This distribution results in the tremendous difference (0.43) of refractive index between alumina (1.76) and zirconia (2.19). Based on the theoretical calculation [2], only the difference of 0.09 in refractive index will lead to significant light scattering and seriously deteriorate the transparency of tetragonal zirconia. Therefore, we conclude that the strong birefringent scattering induced by the distribution of alumina dopant along grain

boundaries causes the low transparency of the TZ-3Y-E sample.

## 4. Conclusions

The effect of alumina dopant on the transparency of tetragonal zirconia has been investigated in this work. Powders of 3% mol yttria stabilized tetragonal zirconia doped with alumina (TZ-3Y-E) are used as starting material to prepare transparent tetragonal  $\text{ZrO}_2$  by high-pressure spark plasma sintering (HP-SPS). The result shows that the addition of alumina dopant deteriorates the transparency although nanometric grains and high density have been achieved in TZ-3Y-E samples. By comparing with the results of tetragonal zirconia without alumina dopant, the low transparency of the TZ-3Y-E samples is induced by the strong birefringent scattering, which is attributed to the distribution of alumina dopant along the grain boundaries of zirconia.

## Acknowledgments

This work was partly supported by the Grant-in-Aid for Scientific Research (B-21360328 and C-22560674) from the Ministry of Education, Culture, Sports, Science and Technology, Japan, and by the Grant-in-Aid for Scientific Research on Priority Areas 474 from the JSPS and the Ministry of Education, Culture, Sports, Science and Technology (MEXT).

## References

- [1] J. Chevalier, L. Gremillard, A. V. Virkar, and D. R. Clarke, "The tetragonal-monoclinic transformation in zirconia: lessons learned and future trends," *Journal of the American Ceramic Society*, vol. 92, no. 9, pp. 1901–1920, 2009.
- [2] J. Klimke, M. Trunec, and A. Krell, "Transparent tetragonal yttria-stabilized zirconia ceramics: influence of scattering caused by birefringence," *Journal of the American Ceramic Society*, vol. 94, no. 6, pp. 1850–1858, 2011.
- [3] P. Duran, P. Recio, J. R. Jurado, C. Pascual, and C. Moure, "Preparation, sintering, and properties of translucent  $\text{Er}_2\text{O}_3$ -doped tetragonal zirconia," *Journal of the American Ceramic Society*, vol. 72, no. 11, pp. 2088–2093, 1989.
- [4] S. R. Casolco, J. Xu, and J. E. Garay, "Transparent/translucent polycrystalline nanostructured yttria stabilized zirconia with varying colors," *Scripta Materialia*, vol. 58, no. 6, pp. 516–519, 2008.
- [5] U. Anselmi-Tamburini, J. N. Woolman, and Z. A. Munir, "Transparent nanometric cubic and tetragonal zirconia obtained by high-pressure pulsed electric current sintering," *Advanced Functional Materials*, vol. 17, no. 16, pp. 3267–3273, 2007.
- [6] H. B. Zhang, Z. P. Li, B. N. Kim et al., "Highly infrared transparent nanometric tetragonal zirconia prepared by high-pressure spark plasma sintering," *Journal of the American Ceramic Society*, vol. 94, no. 9, pp. 2739–2741, 2011.
- [7] K. Matsui, T. Yamakawa, M. Uehara, N. Enomoto, and J. Hojo, "Mechanism of alumina-enhanced sintering of fine zirconia powder: influence of alumina concentration on the initial stage sintering," *Journal of the American Ceramic Society*, vol. 91, no. 6, pp. 1888–1897, 2008.



- [8] Y. Sakka, T. Ishii, T. S. Suzuki, K. Morita, and K. Hiraga, "Fabrication of high-strain rate superplastic yttria-doped zirconia polycrystals by adding manganese and aluminum oxides," *Journal of the European Ceramic Society*, vol. 24, no. 2, pp. 449–453, 2004.
- [9] X. Guo and R. Waser, "Electrical properties of the grain boundaries of oxygen ion conductors: acceptor-doped zirconia and ceria," *Progress in Materials Science*, vol. 151, no. 2, pp. 151–210, 2006.
- [10] K. Matsui, N. Ohmichi, M. Ogai, H. Yoshida, and Y. Ikuhara, "Effect of alumina-doping on grain boundary segregation-induced phase transformation in yttria-stabilized tetragonal zirconia polycrystal," *Journal of Materials Research*, vol. 21, no. 9, pp. 2278–2289, 2006.
- [11] H. Tsubakino, R. Nozato, and M. Hamamoto, "Effect of alumina addition on the tetragonal-to-monoclinic phase transformation in zirconia-3 mol% yttria," *Journal of the American Ceramic Society*, vol. 74, no. 2, pp. 440–443, 1991.
- [12] S. N. B. Hodgson, J. Cawley, and M. Clubley, "Role of Al<sub>2</sub>O<sub>3</sub> impurities on the microstructure and properties of Y-TZP," *Journal of Materials Processing Technology*, vol. 92–93, pp. 85–90, 1999.
- [13] I. M. Ross, W. M. Rainforth, D. W. McComb, A. J. Scott, and R. Brydson, "The role of trace additions of alumina to yttria-tetragonal zirconia polycrystals (Y-TZP)," *Scripta Materialia*, vol. 45, no. 6, pp. 653–660, 2001.
- [14] A. Krell, T. Hutzler, and J. Klimke, "Transmission physics and consequences for materials selection, manufacturing, and applications," *Journal of the European Ceramic Society*, vol. 29, no. 2, pp. 207–221, 2009.
- [15] B. N. Kim, K. Hiraga, K. Morita, H. Yoshida, T. Miyazaki, and Y. Kagawa, "Microstructure and optical properties of transparent alumina," *Acta Materialia*, vol. 57, no. 5, pp. 1319–1326, 2009.
- [16] H. B. Zhang, B. N. Kim, K. Morita, H. Yoshida, J. H. Lim, and K. Hiraga, "Optical properties and microstructure of nanocrystalline cubic zirconia prepared by high-pressure spark plasma sintering," *Journal of the American Ceramic Society*, vol. 94, no. 9, pp. 2981–2986, 2011.
- [17] H. B. Zhang, B. N. Kim, K. Morita, H. Yoshida, J. H. Lim, and K. Hiraga, "Optimization of high-pressure sintering of transparent zirconia with nano-sized grains," *Journal of Alloys and Compounds*, vol. 508, no. 1, pp. 196–199, 2010.
- [18] R. Apeta and M. P. B. van Bruggen, "Transparent alumina: a light-scattering model," *Journal of the American Ceramic Society*, vol. 83, no. 3, pp. 480–486, 2003.
- [19] R. H. French, S. J. Glass, F. S. Ohuchi, Y. N. Xu, and W. Y. Ching, "Experimental and theoretical determination of the electronic structure and optical properties of three phases of ZrO<sub>2</sub>," *Physical Review B*, vol. 49, no. 8, pp. 5133–5142, 1994.
- [20] K. Matsui, H. Yoshida, and Y. Ikuhara, "Phase-transformation and grain-growth kinetics in yttria-stabilized tetragonal zirconia polycrystal doped with a small amount of alumina," *Journal of the European Ceramic Society*, vol. 30, no. 7, pp. 1679–1690, 2010.

